# Synthesis, electrochemical, fluorescence and antimicrobial studies of 2-chloro-3-amino-1,4-naphthoquinone functionalized mononuclear transition metal dithiocarbamate complexes

## Abstract


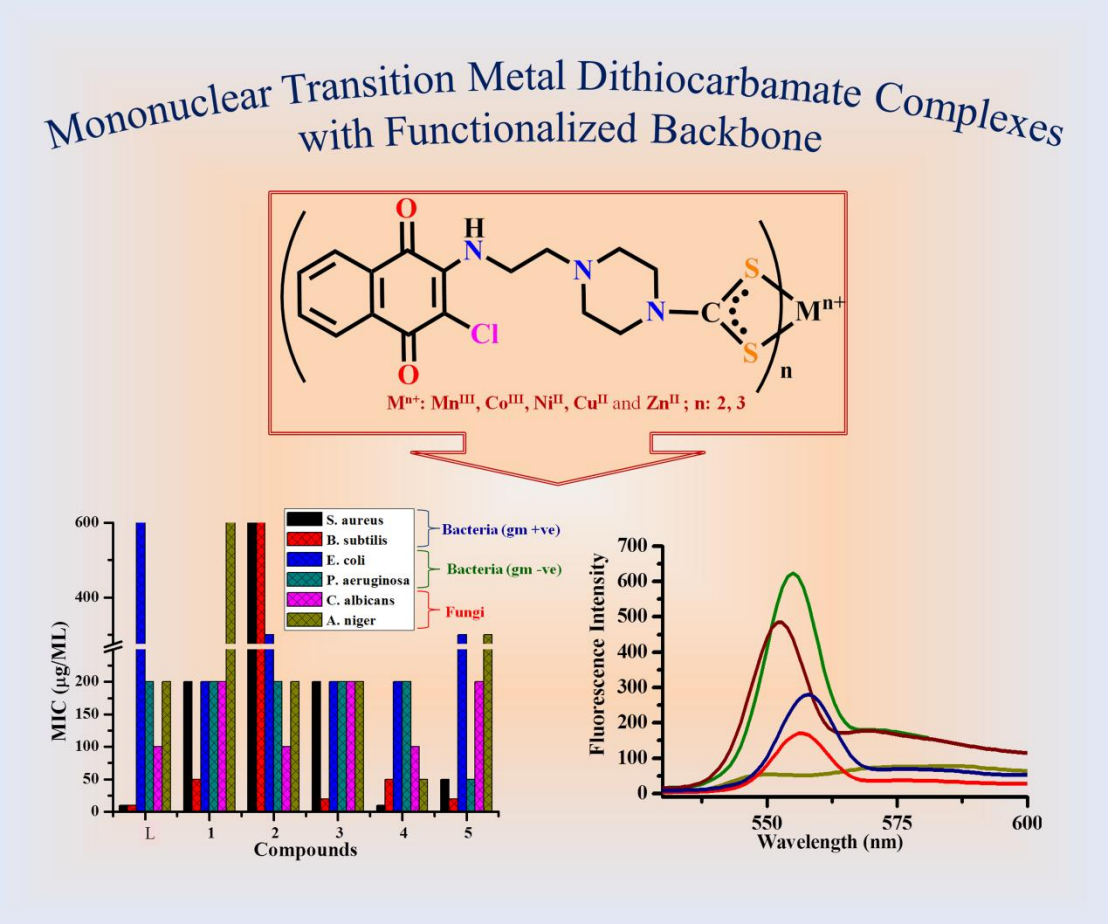


A novel multifunctional ligand 2-chloro-3-{2-(piperazinyl)ethyl}-amino-1, 4-naphthoquinone (**L**) was synthesized by chemo-selective reaction of 2,3-dicholro-1,4-naphthoquinone and 2-(piperazin-1-yl)ethanamine and characterized, prior to use. Mononuclear transition metal dithiocarbamate complexes [M{$\kappa^2$*S*,*S*-$S_2$C-piperazine-$C_2H_4$N(H)ClNQ}$_n$] M = Mn(III) **1**, Co(III) **2**, Ni(II) **3**, Cu(II) **4**, Zn(II) **5**; ClNQ = 2-chloro-1,4-naphthoquinone; n = 2 for **3-5** and n = 3 for **1-2**} bearing pendant 2-chloro-3-amino-1,4-naphthoquinone groups were efficiently synthesized through self-assembly process involving **L**, $\mathbf{CS_2}$ and corresponding metal acetates. **1-5** were characterized by microanalysis and standard spectroscopic methods such as ESI-MS,

IR, $^{1}H$ and $^{13}C$ NMR and UV-visible absorption spectroscopy. Significantly, all compounds exhibit medium to very strong fluorescence emission bands in the visible region with concomitant Stokes shifts of ≈ 280 nm upon excitation at their respective $\lambda_{max}$ values. Thermal stability of complexes **1-5** has been investigated by thermogravimteric analysis. Cyclic voltammetric study clearly reveals that **L** and **1-5** are electro active with respect to the dominant redox-active naphthoquinone moiety and redox active transition metal cations in **1-5** are apparently present in silent mode. Further, **L** and **1-5** were tested against six important pathogen microorganisms *viz.* S. aureus, B. subtilis, E. Coli, *P. Aeruginosa*, C. albicans and A. niger by using the Broth dilution method. A broad spectrum of the strongest antimicrobial activity was determined for the copper(II) complex **4** and **L**. The enhanced antibacterial activity of **L** and copper(II) complex **4** against S. aureus apparently brings them about superior antibacterial agent than the reference drug ciprofloxacin.

## 4B.1. Introduction

Over the decades, transition metal complexes derived from sulphur rich ligands have received a great deal of attention because of their conducting properties, molecular magnetism, electrochemical, optoelectronic properties and biological applications [1-8]. In particular, dithiocarbamates have been emerged as versatile ligands to construct a huge variety of inorganic-organic complex materials with fascination physic-chemical properties, due to their ease of synthesis and ability to bind to a wide range of elements in different oxidation states [9-11]. Since the discovery of first derivative dithiocarbamates *i.e.* tetramethylthiuram disulfide (thiram) [12], which has achieved prominence fungicidal properties, the dithiocarbamate group is considered as a versatile pharmacophore and hence, it is used in the compounds of biological interest [13]. Thermogravimetric studies have been utilized to demonstrate a widespread industrial applications of dithiocarbamate compounds such as foam rubber, fungicides, effective heat stabilizers, antioxidant action, reprocessing of polymers [14].

On the other hand, considerable attention has been paid on the functionalization of naphthoquinone derivatives and evaluation of their biological properties, mainly due to their association in multiple biological oxidative processes [15]. Literature reports suggest that naphthoquinone derivatives possess a wide range

of biological properties that include antibacterial and antifungal, antiviral, antimalarial and anticancer activity which have stimulated the study of these bioactive compounds in the field of medicinal chemistry [16]. However, we could find even a single report on the dithiocarbamate derivatives of naphthoquinone and their transition metal complexes. Although, an enormous number of dithiocarbamate complexes containing simple alkyl/aryl substituents have been synthesized and studied for their various applications, however, functionalization of the ligand backbone is still in its early stage [17].

In the light of these observations, we have designed and synthesized a new secondary amine precursor 2-chloro-3-{2-(piperazinyl)ethyl}-amino-1, 4-naphthoquinone (**L**) which is successfully used to deliver a series of 2-chloro-3-amino-1,4-naphthoquinone functionalized mononuclear transition metal dithiocarbamate complexes **1-5**. All the compounds are thoroughly characterized by microanalysis and standard spectroscopic, optical, thermogravimetric and cyclic voltammetric methods. Further, **L** and **1-5** are screened against a panel of microbes such as *Staphylococus aureus*, *Bacillus subtilis*, *Escherichia coli*, *Pseudomonas aeruginosa*, *Candida albicans* and *Aspergillus niger*. Undoubtedly, the cumulative effect of various pharmacophores present in these compounds resulted into enhanced biological properties.

## 4B.2. Result and discussion

### 4B.2.1. Synthesis and characterization

2-chloro-3-{2-(piperazinyl)ethyl}-amino-1, 4-naphthoquinone (**L**) was synthesized by nucleophilic substitution reaction of 2,3-dichloro-1,4-naphthoquinone with 2-(piperazin-1-yl)ethanamine and characterized. One pot three-component reaction of L, $CS_2$ and $M(OAc)_2$ in $Et_3N$ solvent at room temperature affords access to a new series of mononuclear transition metal dithiocarbamate complexes [M{$\kappa^2$*S*,*S*-$S_2$C-piperazine-$C_2H_4N$(H)ClNQ}$_n$] M = Mn(III) **1**, Co(III) **2**, Ni(II) **3**, Cu(II) **4**, Zn(II) **5**; ClNQ = 2-chloro-1,4-naphthoquinone; n = 2 for **3-5** and n = 3 for **1-2**} bearing pendant 2-chloro-3-amino-1,4-naphthoquinone groups (Scheme 1). The required dithiocarbamate derivative of L was synthesized *in situ*. Complexes **1-5** display moderate to poor solubility in common organic solvents, however, there are fairly soluble in DMSO/ DMF, solvents of high nucleophilicity. These are found to be air-

stable in solid state and in the solution over a period of days. Our attempts to grow single crystals suitable for single crystal X-ray diffraction study were unsuccessful.

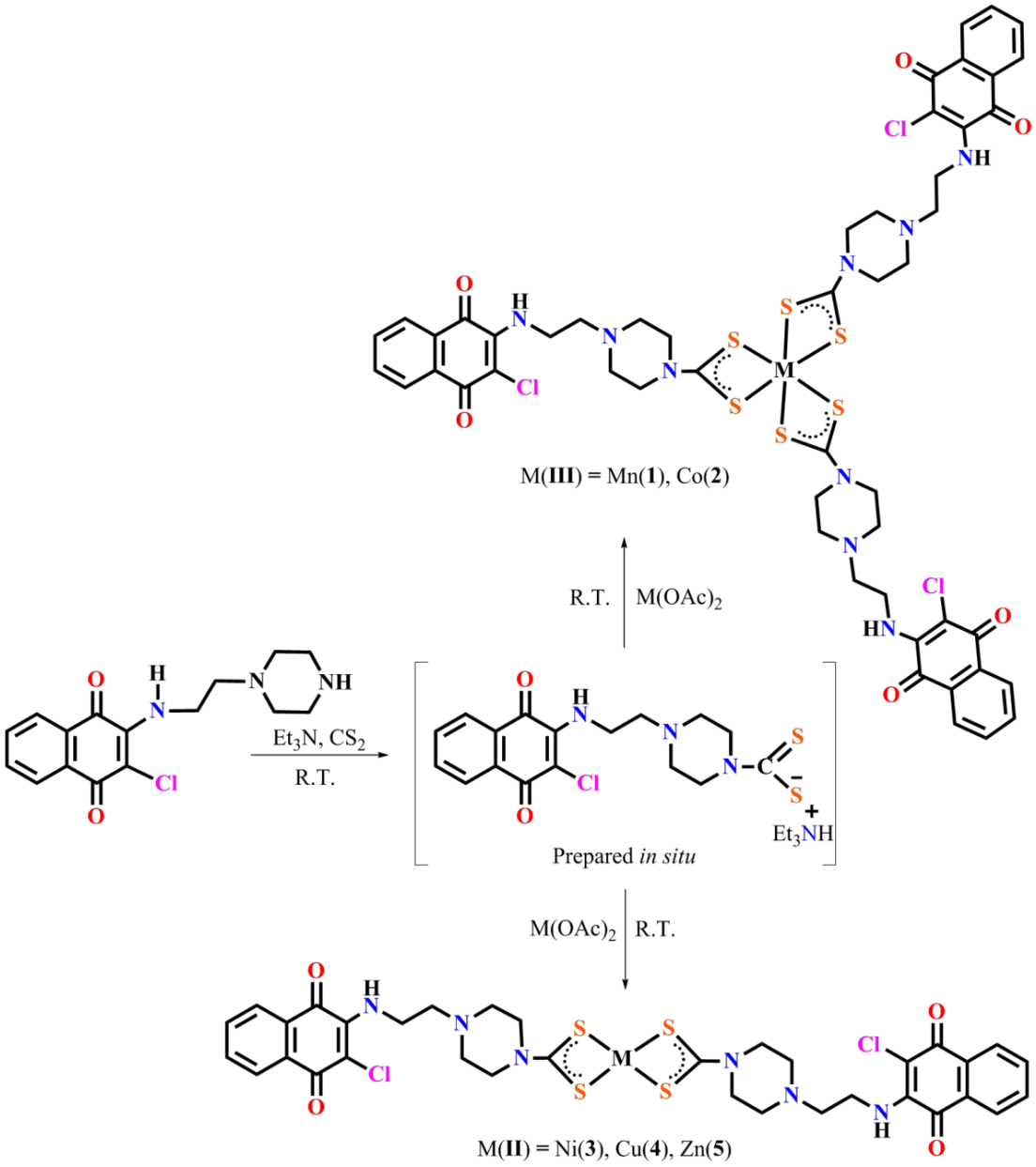


**Scheme 1:** Preparation of monometallic dithiocarbamate complexes.

It has been experienced by us [18] and Professor Hogarth's research group [19] that transition metal dithiocarbamate complexes with functionalised backbones are easy to synthesize but their crystallization can be more problematic. **L** and **1-5** were characterized by microanalysis, standard spectroscopy viz. ESI MS, FT-IR, $^{1}H$ and $^{13}C$ NMR, UV-visible absorption, emission and by thermogravimetric methods. The ESI-MS of the complexes **3** and **5** gave molecular ion peaks at m/z 849.3 and 856.1

respectively, which corresponds to $[M+H]^+$ along with differential fragmentation peaks (supplementary information).

### 4B.2.2. IR spectral study

The IR spectrum of L displays characteristic υ(N-H) bands at 3320 and 3252 $cm^{-1}$due to presence of naphthoquinone-conjugated amine and piperazinyl amine groups, respectively. While a strong band at 1677 $cm^{-1}$ arises due to υ(C=O) stretch of naphthoquinone moiety.

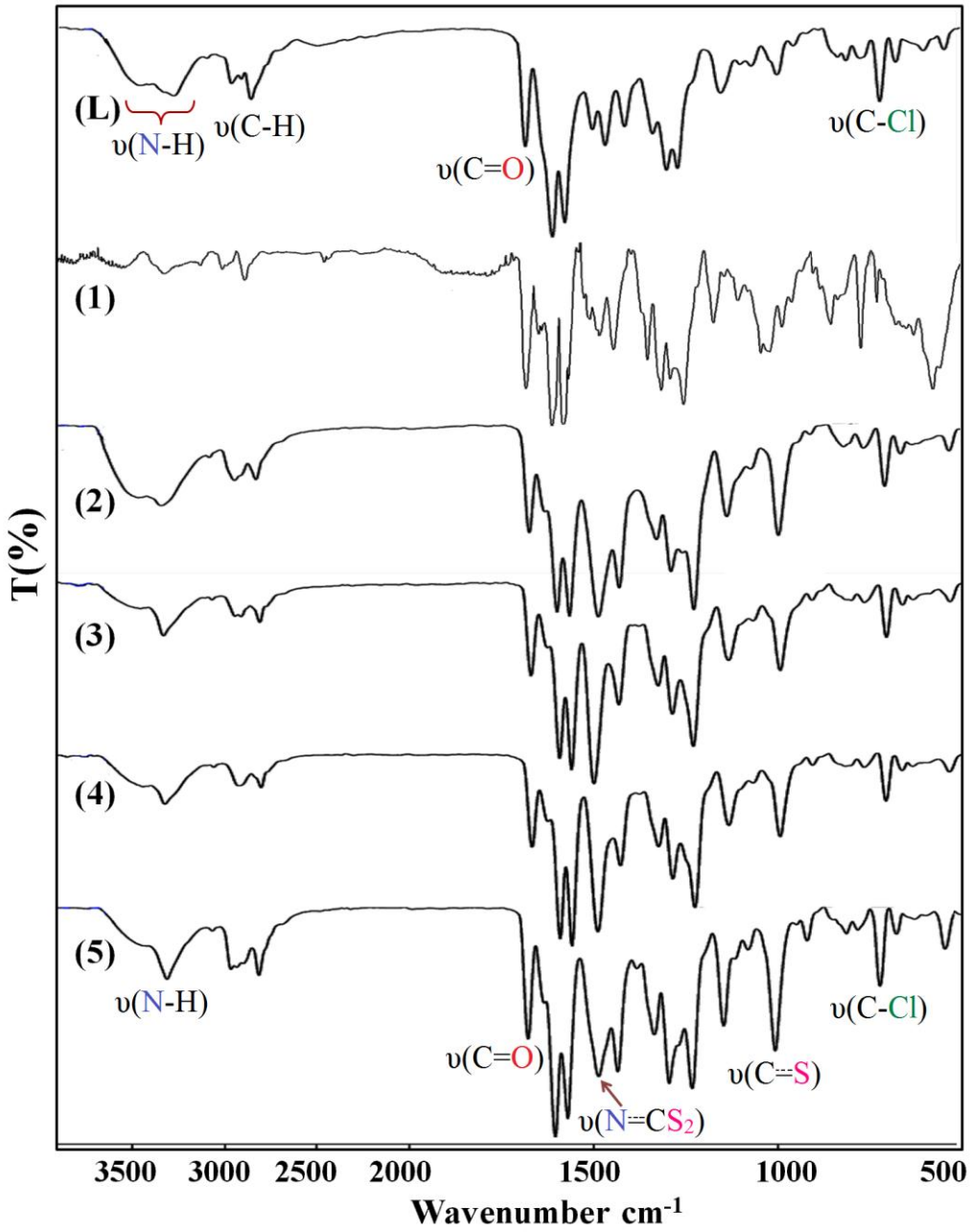


**Fig. 1.** IR Spectrum of 2-chloro-3-{2-(piperazinyl)ethyl}-amino-1, 4-naphthoquinone (**L**) and its dithiocarbamate complexes **1-5**.

The IR spectra of **1-5** clearly showed the disappearance of one of the υ(N-H) band associated with piperazinyl amine and the appearance of two new single sharp medium intensity bands in 1427-1498 $cm^{-1}$ and 1006-1010 $cm^{-1}$ regions due to υ(N-$CS_2$) and υ(C-S) stretching vibrations. These are two regions of particular interest in the IR spectral study of dithiocarbamates complexes and confirm the bidentate coordination of dithiocarbamate lignads. [20] The observed ν(N-$CS_2$) stretchings for **1-5** are indeed intermediates of C=N double bond and C-N single bond stretchings, arises due to the mesomeric drift of the electron cloud of the dithiocarbamate (–$NCS_2$) moiety towards the metal ion and confirmed an increase in the C–N double bond character. Notably, the naphthoquinone-conjugated amine band υ(N-H) along with υ(C=O) and υ(C-Cl) bands for complexes **1-5** remain present almost at the same positions *viz.* 3320, 1677 and 722 $cm^{-1}$ respectively, compared to their positions in $L^1$ (Fig. 1). This gives a strong evidence for the presence of pendent 2-chloro-3-amino-1,4-naphthoquinone groups in **1-5** which is further confirmed by NMR study.

### 4B.2.3. NMR spectral study

The $^1$H NMR spectrum of precursor **L** recorded in $CDCl_3$ display most characteristic signals at δ 2.51 ppm and 6.74 ppm due to piperazinyl and naphthoquinone-conjugated –NH protons, whereas signals appeared in 3.91-2.62 ppm and 8.09-7.545 ppm regions are attributed to the aliphatic methylene and aromatic protons, respectively. The $^{13}$C NMR spectrum of **L** in $CDCl_3$ displays characteristic signals due to ketonic groups (>C=O) of naphthoquinone at 180.66, 176.71 ppm along with expected signals in aromatic/aliphatic regions. For comparison purpose, *in situ* prepared triethylammonium salt of a dithiocarbamate derivative of L was also characterized by $^1$H and $^{13}$C NMR spectra (Supporting Information). The $^{13}$C NMR spectrum displays most characteristic signal at 193.69 ppm due to –$NCS_2$ moiety and confirms the formation of dithiocarbamate derivative of L *in situ*. In the $^1$H NMR spectra of complexes **3** and **5**, characteristic piperazinyl –NH signal is disappeared and a significant downfiled shifting of aromatic/ aliphatic signals was observed when compared to their respective positions in L (supporting information). The $^{13}$C NMR spectrum of **5** displays a very downfield signal at ~203 ppm, a characteristic feature of coordinated dithiocarbamate moiety derived from secondary amines [21]. Notably, the signals due to ketonic groups (>C=O) of naphthoquinone appear almost at same

positions *viz.* δ =180.85 and δ = 176.77 ppm when compared to their positions in L. This confirms the non-involvement of ketonic groups in complexation. The assignments of $^{1}H$ and $^{13}C$ signals are supported by DEPT 135 NMR spectral study, which can be clearly distinguished the aromatic carbons (appear in the positive region) from aliphatic methylene carbons (appear in negative region). The position and features of the NMR signals confirm the purity and composition of the complexes and also reveal that no ligand-exchange reaction occurs in solution.

### 4B.2.4. Electronic absorption spectral and magnetic moment studies

The electronic emission spectral data of **L** and its mononuclear dithiocarbamate complexes **1-5** were investigated at room temperature from $10^{-5}$ M DMSO solution samples and the pertinent results are summarized in Table 1. The assignment of UV-visible absorption bands are based on the literature reports on closely related compounds. [22, 23, 24] The UV-visible absorption spectra of **L** and **1-5** displayed expected benzene and naphthoquinone bands in 275–277 nm and 324–340 nm regions mainly arises due to π→π* electronic transitions [22]. In addition, a low energy broad band is observed in the visible regions between 443-468 nm, assignable to CT transitions and weak n→π* transitions of the carbonyl group of the quinone [25]. Notably, this broad band in the visible region for all the complexes **1-5** showed a significant hypsochromic shift (blue shift) relative to its position in **L (**Fig. 2). A new band clearly seen at 389 nm in the electronic absorption spectrum of nickel complex **3**, probably arises due to intra ligand charge transfer transitions associated with N–C=S group of coordinated dithiocarbamate ligands. Similar band for other complexes is expected, however, it could not be seen due to broad nature of the band arises from the carbonyl group of the quinone (vide supra). Further, cobalt(III) complex **2** exhibits a weak absorption band at ~ 649 nm which is consistent with the absorption behavior of [Co{$\kappa^2$S,S-$S_2$C-piperazine-$C_2H_4$N=C(Ph)}$_3$] [18] and other cobalt(III) complexes. [26] The UV-visible absorption behavior of copper(II) **3** and nickel(II) **4** complexes are quite similar to those of closely related compounds [18, 27]. The Zn(II) complex **5** is of white colour and presents a featureless electronic spectrum. Unlike manganese(II)-bis-dithiocarbamate complexes [28], the manganese(III) complex **1** is of light pink colour and stable in the solution and in solid state. Literature report [29] suggests the existence of divalent Mn($R_2$dtc)$_2$ species as yellow solids which are

highly unstable and readily oxidize to the dark-violet trivalent complexes $Mn(R_2dtc)_3$. Moreover, the *d-d* bands of high-spin Mn(III) complexes possesses extremely low intensity and in the presence of organic ligands and they could rarely be detected [30]. The magnetic moment values (Table 1) along with UV-visible absorption bands suggest an octahedral environment around manganese(III)/ cobalt(III), the square planar environment around nickel(II)/copper(II) and tetrahedral environment around zinc(II) in their respective mononuclear dithiocarbamate complexes **1-5**.

### 4B.2.5. Fluorescence emission spectral study

The fluorescence properties of **L** and its dithiocarbamate complexes **1-5** were studied at room temperature (298 K) from $10^{-5}$M DMF solution samples and the spectral data is summarized in Table 3. The fluorescence spectra of these are shown in (Fig. 3). Apparently all compounds exhibit medium to very strong fluorescence emission bands in the visible region upon excitation at their respective $\lambda_{max}$ values.

**Table 1**. UV-visible, Magnetic and Fluorescence spectral data of compounds $10^{-5}$ M in DMF solution

| Entry | $\lambda_{max}$ nm ($\varepsilon$, $LMol^{-1}cm^{-1}$) | Wave number $cm^{-1}$ | Magnetic moment $\mu_{eff}$ (BM) | Fluorescence spectral data $\lambda_{ex}$ (nm) | $\lambda_{em}$ nm (Intensity) |
|---|---|---|---|---|---|
| L | 277 (65608) π→π* | 36101 | -- | 277 | 557 (280) π*→π |
| | 335 (10998) sh, π→π* | 29850 | | | |
| | 487 (14902) n→π* | 20533 | | | |
| 1 | 276 (73761) π→π* | 36231 | 4.95 | 276 | 557 (129) π*→π |
| | 340 (13254) sh, π→π* | 29411 | | | |
| | 465 (10178) n→π* | 21505 | | | |
| 2 | 277 (75010) π→π* | 36101 | Dia | 277 | 556 (172) π*→π |
| | 324 (32041) sh, π→π* | 30864 | | | |
| | 468 (8536) n→π* | 21367 | | | |
| | 649 (1365) d-d | 15408 | | | |
| 3 | 276 (50550) π→π* | 36231 | Dia | 276 | 555 (621) π*→π |
| | 324 (49915) π→π* | 30864 | | | |
| | 389 (14902) n→π* | 25706 | | | |
| | 460 (8536) n→π* | 21739 | | | |
| 4 | 275 (65608) π→π* | 36363 | 1.91 | 275 | 552 (481) π*→π |
| | 333 (8808) sh, π→π* | 30030 | | | |
| | 443 (13629) n→π* | 22573 | | | |
| 5 | 275 (80029) π→π* | 36363 | Dia | 272 | 547 (53) π*→ π |
| | 339 (7031) sh, π→π* | 29498 | | | 576 (76) π*→ π |
| | 465(8536) n→π* | 21505 | | | |

For instance, **L** and **1-5** fluoresces strongly at ~550 nm with concomitant Stokes shifts of ≈ 280 nm, except zinc complex **5** which shows a weak broad fluorescence emission band at 547 upon excitation at 272 nm. The weak fluorescence behaviour of zinc complex **5** is somewhat in contrast to many other zinc complexes that are shown to exhibit maximum fluorescence emissions upon excitation at lower wavelengths. [18, 31] Contrarily [32], complexes **3** and **4** showed excellent fluorescence emission behaviour upon excitation of intra ligand charge transfer bands. Such a trend of fluorescence spectra and concomitant bathochromic shifts of intramolecular charge-transfer emissions by coordination compounds were previously observed in dithiocarbamate [33] complexes. The fluorescence bands appeared in the spectra of all the complex **1-5** are attributed to $\pi^* \rightarrow \pi$ transitions. None of the compounds display any noticeable fluorescence upon excitation at their low energy bands such as 487, 465, 468, 460, 443 and 465 nm, respectively.

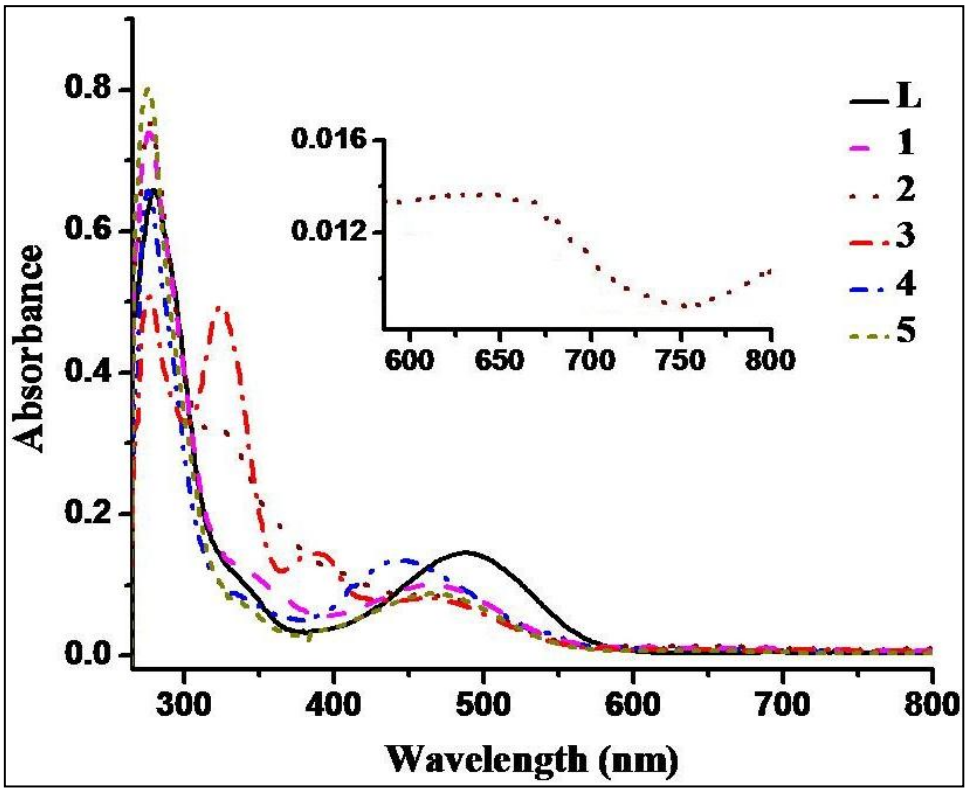


**Fig. 2.** UV-visible absorption spectra of the Ligand and dithiocarbamate metal complexes at room temperature in $10^{-5}$ M DMF solution

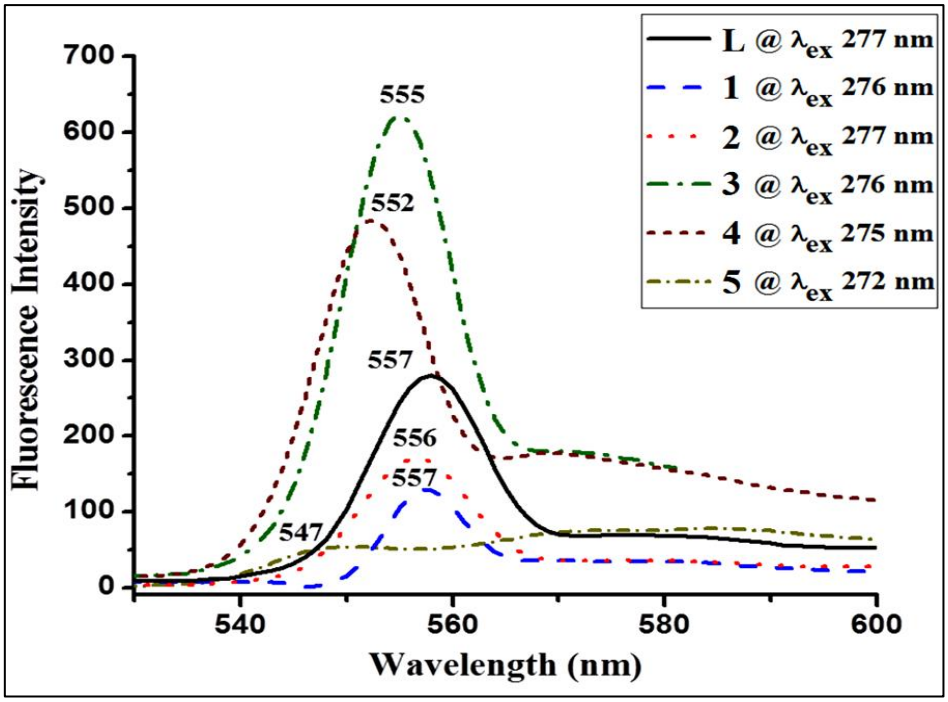


**Fig. 3.** Fluorescence spectra of the Ligand and dithiocarbamate metal complexes at room temperature in $10^{-5}$ M DMF solution

### 4B.2.6. Cyclic Voltammetric Study

Since a large part of the biological activity of naphthoquinone derivatives is related to their electron-transfer ability, [15] it becomes pertinent to investigate the electrochemical behaviour of these newly synthesized compounds. Electrochemical investigations of **L** and **1-5** were performed using cyclic voltammetry in the potential range of +2.1 to -2.1 V from 1.0 mM $CH_2Cl_2$ solutions containing n-$Bu_4NPF_6$ (0.1 M) as supporting electrolyte at a scan rate of 100 $mVs^{-1}$. The voltammograms for these are shown in Fig 4 and electrochemical data is represented in **Tables 2**. The electrochemical examination of **1-5** clearly demonstrates the quasi-reversible redox behavior of **L**, **1** and **5**. First, electrochemical examination of **L** clearly demonstrates its quasi-reversible redox behavior. It primarily exhibits two single-electronic waves due to eletcroredution of naphthoquinone moiety to semiquinone radical anion and then to dianion, respectively. The separation between each cathodic and corresponding anodic peak, ΔEp at 100 mV/s scan rate is larger than 59 mV (Table 2) and the ratio of the current intensity of the cathodic and anodic peaks are different from unity, suggesting a quasi-reversible nature of both the redox couples of **L**. Compared to the cyclic voltammogram of **L**, its complexes **1-5** did not display any

additional peak, in the cathodic or anodic scan under the similar experimental conditions, *i.e.* voltammograms of **1-5** exhibit similar feature, except the differences in the cathodic/anodic current peak heights (Fig. 9). This implies that the complexes **1-5** are primarily electro active with respect to the dominant redox-active naphthoquinone moieties. The redox active transition metal cations in the dithiocarbamate complexes **1-5** are apparently present in silent mode. The silent nature of transition metal ions in the presence of dominant electro-active ligands has previously been observed in a number of cases. [10b, 18, 34]

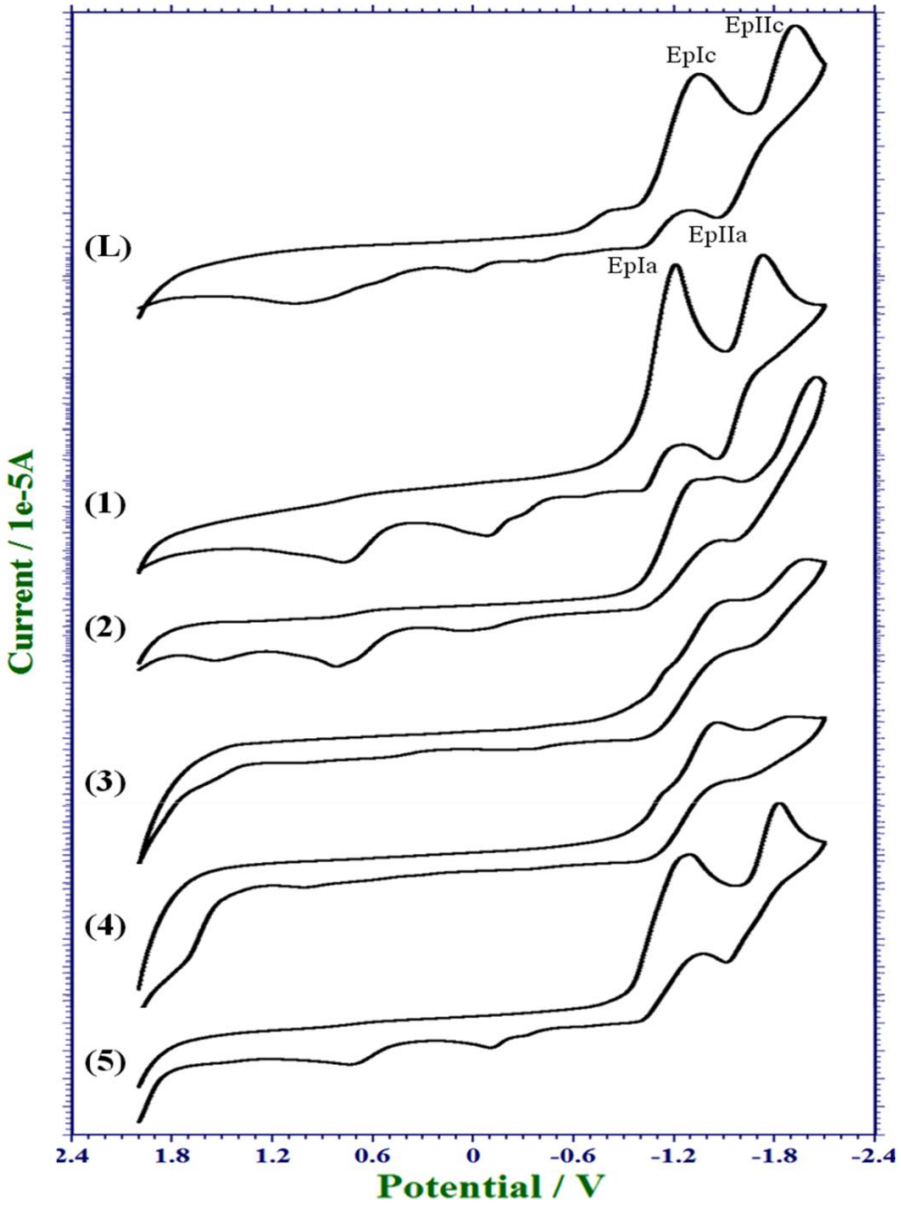


**Fig. 4.** Cyclic voltammograms of a 1 mM solution of ligand precursor **L** and compounds **1-5** in $CH_2Cl_2$ containing 0.1 M tetra-n-butylammonium hexafluorophosphate as the supporting electrolyte.

Further, electrochemically equivalence of multiple naphthoquinone units of **1-5** is confirmed by the emergence of a single quasi-reversible wave. When compared the electrochemical responses of these complexes with corresponding ligand precursor **L**, complexes **1** and **5** exhibit redox potentials that are significantly shifted anodically whereas the redox potentials of the rest of the complexes are shifted cathodically.

**Table 2** Electrochemical data for the compounds **L** and **1-5**

| Entry | $Ep_{Ic}$(V) | $Ep_{IIc}$(V) | $Ep_{Ia}$(V) | $Ep_{IIa}$(V) | $\Delta Ep_I$(V) ($E_{pI,a}$– $E_{pI,c}$) | $\Delta Ep_{II}$(V) ($E_{pII,a}$– $E_{pII,c}$) |
|---|---|---|---|---|---|---|
| L | -1.350 | -1.923 | -1.013 | -1.468 | 0.337 | 0.455 |
| 1 | -1.210 | -1.730 | -1.008 | -1.456 | 0.202 | 0.274 |
| 2 | -1.469 | -2.046 | -0.995 | -1.550 | 0.474 | 0.496 |
| 3 | -1.491 | -1.969 | -1.008 | -1.639 | 0.483 | 0.330 |
| 4 | -1.462 | -1.887 | -1.037 | -1.627 | 0.425 | 0.260 |
| 5 | -1.291 | -1.834 | -0.995 | -1.515 | 0.296 | 0.319 |

### 4B.2.7. Biological evaluation

The development of new antimicrobial agents is of considerable interest because of unprecedented increase of multidrug resistance in common pathogens and the hasty appearance of new infections. Reports suggest that a major part of fatal nosocomial infection as well as community-acquired infections are caused by S. aureus and P. aeruginosa [35]. While the most prominent fungal pathogens affecting human being through invasive candidiasis [36] is C. albicans. The spread of these organisms in healthcare settings is often difficult to control due to the presence of multiple intrinsic and acquired mechanisms of antimicrobial resistance. Thus, it becomes necessary to investigate the biological significance of newly synthesized compounds.

The ligand precursor **L** and its dithiocarbamate transition metal complexes **1-5** were screened by Broth dilution method [37] for their *in vitro* antibacterial activity against two gram positive bacteria S. aureus, B. subtilis, and two gram negative bacteria E. coli, P. aeruginosa. They were also evaluated for their *in vitro* antifungal activity against C. albicans and A. niger. Concentration of compounds was ranging from 10 µg to 600 µg (Fig. 5). The lowest concentrations of the compounds that prevented visible growth are provided in Table 3. It was established that the solvent had no antibacterial or antifungal activities against any of the test microorganisms.

Ciprofloxacin and Flucanazole were used as standard reference drugs and these were tested under the similar conditions for comparison.

**L** and its dithiocarbamate complexes **1-5** exhibit moderate to excellent activity against all the tested bacteria (Table 3), except the activity of **L** (MIC = 600 $\mu gml^{-1}$) against E. coli, a gm -ve bacteria and activity of cobalt(III) complex **2** (MIC = 600 $\mu gml^{-1}$) against both of the gm +ve bactria. In particular, **L** (MIC <10 $\mu gml^{-1}$ against S. aureus and B. subtilis) and copper(II) complex **4** (MIC 10 $\mu gml^{-1}$ against S. aureus) exhibit a remarkable activity (Fig. 5 and Fig. 6). In fact, a very good antibacterial activity of copper(II) **4** and zinc(II) **5** complexes were found against both of the gram positive bacteria S. aureus and B. subtilis whereas Mn(III) **1**, Ni(II) **3** complexes displayed good activity only against B. subtilis. All the compounds displayed moderate activity against both of the gm -ve bacteria, except **5** which showed very good activity against P. aeruginosa. Apart from this, compounds **L** and **1-5** showed moderate activity against both of the fungi (Figure xx), except manganese(III) complex **1** (poor; MIC = 600 $\mu gml^{-1}$)and copper(II) complex **4** (very good; MIC = 50 $\mu gml^{-1}$) against A. niger. The enhanced antibacterial activity of **L** and copper(II) complex **4** against S. aureus (Table 3) apparently bring them about superior antibacterial agent than the reference drug ciprofloxacin.

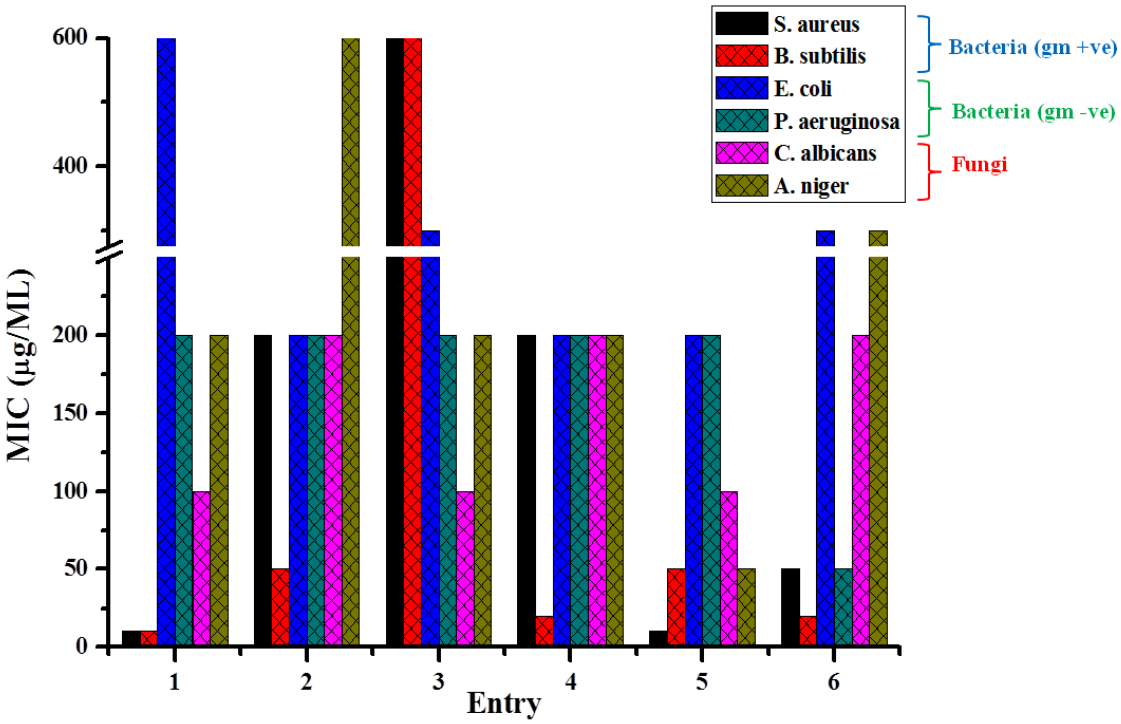


**Fig. 5.** Antimicrobial MIC ($\mu gml^{-1}$) values for **L** and its dithiocarbamate complexes **1-5**.

The activity of these compounds may either be associated with cell wall destruction, DNA damage [38], protein synthesis inhibition or chelation with metal ions present in fungal cells, thus grudging them of the needed ions which would lead to cell mortality [39].

**Table 3** MIC determination of antibacterial and antifungal agent (µg)

| Entry | MIC ($\mu gml^{-1}$) | | | | | |
|---|---|---|---|---|---|---|
| | Bacteria (gm +ve) | | Bacteria (gm –ve) | | Fungi | |
| | S. aureus | B. subtilis | E. coli | P. aeruginosa | C. albicans | A. niger |
| L | <10 | <10 | 600 | 200 | 100 | 200 |
| 1 | 200 | 50 | 200 | 200 | 200 | >600 |
| 2 | 600 | 600 | 300 | 200 | 100 | 200 |
| 3 | 200 | 20 | 200 | 200 | 200 | 200 |
| 4 | 10 | 50 | 200 | 200 | 100 | 50 |
| 5 | 50 | 20 | 300 | 50 | 200 | 300 |
| Ciprofloxacin | 15 | 5 | 15 | 10 | - | - |
| Flucanazole | - | - | - | - | 10 | 40 |

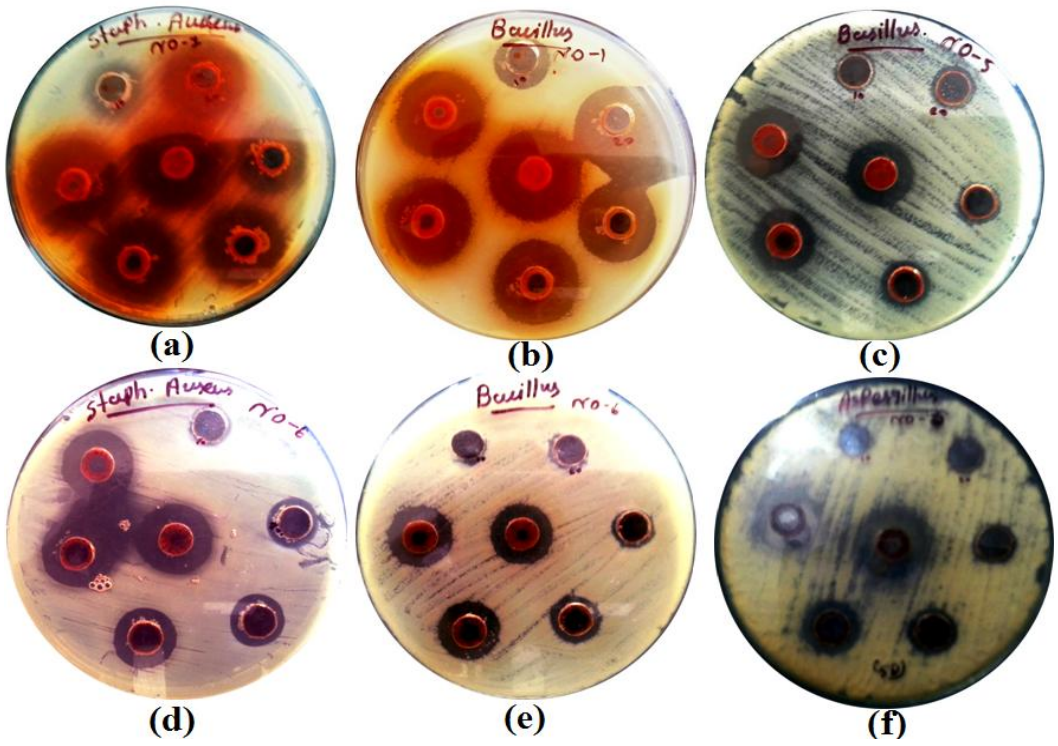


**Fig. 6**. Zone of inhibition of ligand precursor **L** against (a) S. Aureus, (b) B. Subtilis; **3** against (c) B. Subtilis; **4** against (d) S. aureus, (e) B. subtilis and (f) A. niger in different concentration ranging from 10 µg to 600 µg/ml in DMSO solution.

### 4B.2.8. TG/DTA study

Mononuclear transition metal dithiocarbamate complexes **1-5** were further studied by thermogravimetric method to investigate their thermal decomposition patterns in the temperature ranges from room temperature to 750 ºC. Rightfully, the heating rate was controlled at 10 ºC $min^{-1}$ under nitrogen atmosphere. The temperature range and percentage weight loss during the decomposition as well as the temperature corresponding to the maximum rate of decomposition are summarized in Table 4. Thermogravimetric plots for these compounds (Fig. 7) clearly reveals a single or multi stage mass loss on DTG curves and corresponding DTA peaks, attributed to endothermic and/or exothermic elimination of molecular fragments due to the thermal degradation. It may be noted that the thermal decompositions of all the complexes **1-5** starts before their melting points and accompanied by the appearance of one or more endothermic peak on corresponding DTA curves. Further, it appears that manganese(III) complex 1 and zinc complex **5** are thermally unstable and their degradations start at a lower temperature (120-140 ºC), compared to other complexes which are indeed stable up to ~200 ºC. All the complexes exhibit only ≈50% of degradations on TG curves and a stable residual mass could not be obtained up to 750 ºC. Remarkably, thermal decompositions of zinc(II) complex **5** is essentially taking place in two stages. The first stage starts at 120 °C with a quick mass loss of 8.9 % on TG curve which corresponds to the loss of $CS_2$ molecule (calc. 8.8%). The second stage starts at 151 °C and only 48.1 % mass loss was observed on TG curve up to 750 °C. It gives a maximum rate of decomposition of 0.166 mg $min^{-1}$ on DTG curve.

**Table 4** Thermogravimetric data of the dithiocarbamate metal complexes **1–5**

| Entry | Steps | Temp. range (°C) | Weight loss (%) | DTA peak (°C) | DTG peak (°C) | Rate of decomposition (mg $min^{-1}$) | Residual mass (%) found |
|---|---|---|---|---|---|---|---|
| **1** | I | 140-750 | 35.4 | 190.2 | 177.1 | 0.078 | 64.6 |
| **2** | I | 230-750 | 46.3 | 222.5 | 240.4 | 0.239 | 53.7 |
| | | | | 270.2 | 264.6 | 0.237 | |
| **3** | I | 240-750 | 53.4 | 234.9 | 244.4 | 0.306 | 46.6 |
| | | | | 309.5 | 309.5 | 0.505 | |
| **4** | I | 190-750 | 47.5 | 234.2 | 196.5 | 0.165 | 52.5 |
| | | | | | 225.2 | 0.242 | |
| **5** | I | 120-130 | 8.9 | 210.0 | 125.3 | 0.120 | 51.9 |
| | II | 151-750 | 39.2 | | 212.4 | 0.166 | |

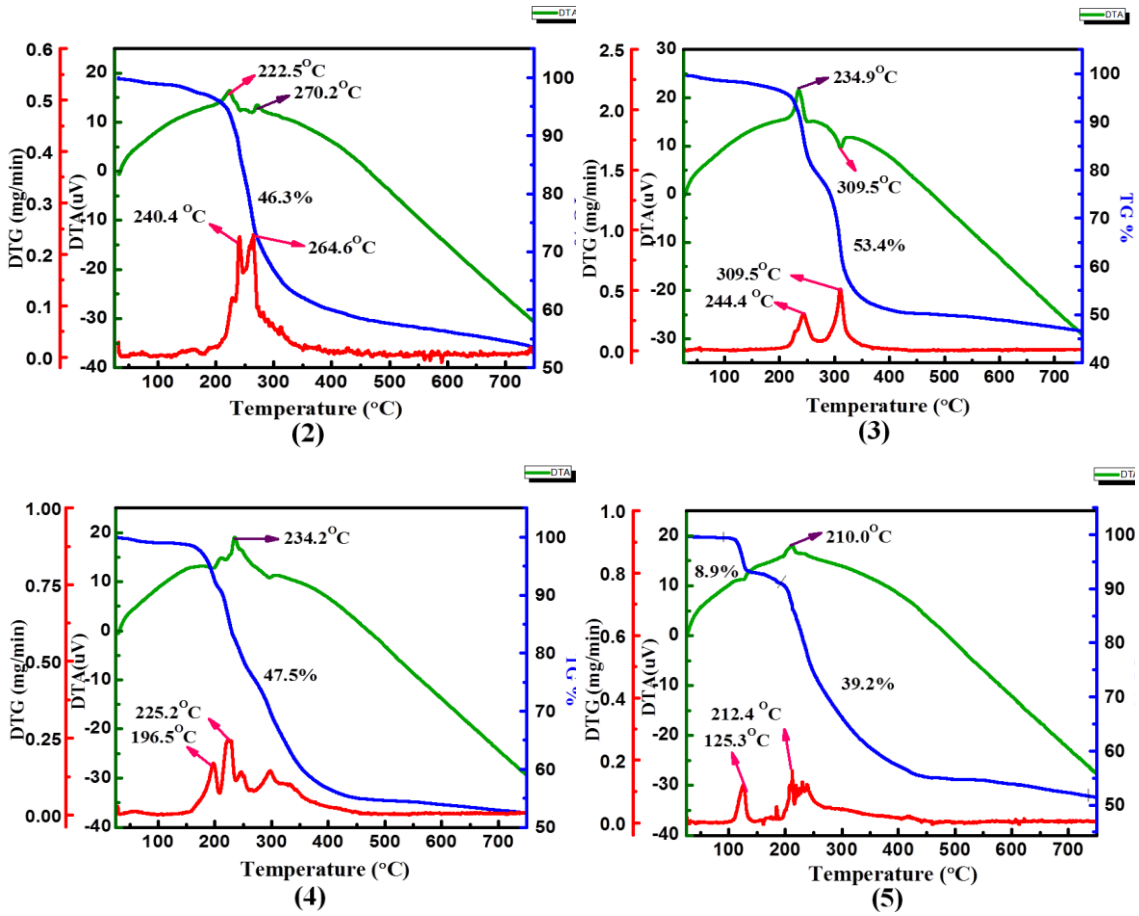


**Fig. 7.** TG/DTA curves of the dithiocarbamate metal complexes **2-5**.

## 4B.3. Conclusion

In conclusion, a novel multifunctional ligand 2-chloro-3-{2-(piperazinyl)ethyl}-amino-1, 4-naphthoquinone (**L**) was synthesized and successfully used to obtain [M{$\kappa^2$*S*,*S*-$S_2$C-piperazine-$C_2H_4$N(H)ClNQ}$_n$] M = Mn(III) **1**, Co(III) **2**, Ni(II) **3**, Cu(II) **4**, Zn(II) **5**; ClNQ = 2-chloro-1,4-naphthoquinone; n = 2 for **3-5** and n = 3 for **1-2**} in a single step involving self-assembly of **L**, $\mathbf{CS_2}$ and corresponding metal acetates. **L** and complexes **1-5** bearing functionalized ligand backbones were characterized satisfactorily by microanalysis and standard spectroscopy. Significantly, complexes **3** and **4** showed excellent fluorescence emission behaviour upon excitation of intra ligand charge transfer bands with concomitant Stokes shifts of ≈ 280 nm. **L** and **1-5** are electro active with respect to the dominant redox-active naphthoquinone moiety and redox active transition metal cations in **1-5** are apparently present in silent mode. A broad spectrum of the strongest antimicrobial activity was determined for the copper(II) complex **4** and **L**. Interestingly, the enhanced antibacterial activity of **L** (MIC <10 $\mu gml^{-1}$) as well as copper(II) complex **4** (MIC 10 $\mu gml^{-1}$) against S. aureus

apparently brings them about potent antibacterial agent than the reference drug *Ciprofloxacin* (MIC 15 $\mu gml^{-1}$).

## 4B.4. Experimental section

### 4B.4.1. Materials and measurement

All solvents were purchased from the commercial sources and were freshly distilled prior to use. All the reagents such as metal acetates $Mn(OAc)_2.4H_2O$, $Co(OAc)_2.4H_2O$, $Ni(OAc)_2.4H_2O$, $Cu(OAc)_2.H_2O$, $Zn(OAc)_2.2H_2O$ and $CS_2$ were purchased from Merck and Sigma-Aldrich Chemicals Limited and these were used without further purification. Elemental analyses (C, H, N) were carried out on a Perkin-Elmer 2400 analyzers. Thin Layer Chromatography was performed on Merck 60 F254 Aluminium coated plates. Magnetic moments were done by Faraday Valance-2002 (1.0Tesla), balance-Mettler UMx5, temperature controller OMEGA. FT-IR spectra were recorded in the 4000-400 $cm^{-1}$ range using a Perkin-Elmer FT-IR spectrometer as KBr pellets. The $^{1}H$ and $^{13}C$ NMR spectra of relevant compounds were obtained on a Bruker AV-III 400 MHz spectrometer in spectrometer with $CDCl_3$ and DMSO-*d6* as solvent and TMS as internal standard. Mass spectrum of L was recorded on Thermo-Fischer DSQ II GCMS instrument while ESI MS were obtained from AB SCIEX, 3200 Q TRAP LC/MS/MS system. UV-visible spectra were recorded on a Perkin Elmer Lambda 35 UV-visible spectrophotometer and the optical characterization of solid samples was performed by using the UV-visible transmittance measurements. Fluorescence was recorded on JASCO make spectrofluorometer model FP-6300. TGA/DTA plots were obtained using SII TG/DTA 6300 in flowing $N_2$ with a heating rate of 10 °C $min^{-1}$. The antimicrobial activity was performed by Division of Centralnkashiba, Advanced diagnostic laboratory, Surat, India.

### 4B.4.2. Synthesis of 2-chloro-3-{2-(piperazinyl)ethyl}-amino-1, 4-naphthoquinone (L)

The rapid interaction between 2, 3-dichloro-1,4-naphthoquinone (DClNQ) (1.0 g, 4.404 mmol) and 2-(piperazin-1-yl)ethanamine (0.568 ml, 4.404 mmol) in 30 ml of ethanol, the reaction mixture was allowed to stir for 4-6 hours at room temperature. A change in colour from yellow to red of reaction mixture was observed. The reaction mixture was dried in rotatory evaporator and basify with saturated solution of

$Na_2CO_3$. Filter it and washed with distilled water 2-3 times and dried in desiccators over calcium chloride to yield the pure product of red colour. $^1$H NMR (400 MHz, $CDCl_3$): $\delta$ 8.09-8.07 (dd, 1H, *Ph*), 7.97-7.95 (dd, 1H, *Ph*), 7.68-7.64 (td, 1H, *Ph*), 7.58-7.545 (td, 1H, *Ph*), 6.74( s, 1H, *N-H*), 3.91-3.87(m, 2H, $CH_2$), 3.06 (t, 2H, $CH_2$), 2.66-2.62(m, 8H, $CH_2$), 2.51( s, 1H, *N-H*). $^{13}$C NMR (400 MHz, $CDCl_3$): $\delta$ 180.66(C=O), 175.71(C=O), 148.05(C-N), 134.82, 134.72, 132.76, 132.34, 131.97, 126.74, 126.69, 126.24, 126.18, 56.81, 55.66, 53.93, 53.68, 46.10, 45.99, 40.83, 38.51; $^{13}$C DEPT 135 NMR (400 MHz, $CDCl_3$): $\delta$ 134.91, 132.46, 126.73, 126.69, 56.37, 52.99, 52.29, 51.80, 45.67, 44.62, 40.85, 40.74, 39.99. Full MS (m/z): 319.32 $[M]^+$, calcd. Mass: 319.1 $[M]^+$.

### 4B.4.3. Synthesis of triethylammonium dtc salt of 2-chloro-3-{2-(piperazinyl)ethyl}-amino-1, 4-naphthoquinone

The ligand precursor 2-chloro-3-{2-(piperazinyl)ethyl}-amino-1, 4-naphthoquinone (**L**) (0.319 g, 1.0 mmol) was dissolved in 20 ml of triethyl amine and then $CS_2$ (0.114 g, 1.5 mmol) after 30 minutes were added. The mixture was stirred for 1hr and then after dry the solvent by rotatory evaporator got the solid product. The residue was dried in high vacuum and the solid product was stored in 10-20 ºC under nitrogen atmosphere. $^1$H NMR (400 MHz, $CDCl_3$): $\delta$ 8.17-8.15 (dd, 1H, *Ph*), 8.05-8.03 (dd, 1H, *Ph*), 7.76-7.71 (td, 1H, *Ph*), 7.66-7.64 (td, 1H, *Ph*), 6.95( s, 1H, *N-H*), 4.53(m, 2H, $CH_2$), 4.01 (t, 2H, $CH_2$), 3.21-3.09(m, 8H, $CH_2$), 2.75-2.58(q, 6H, $CH_2$), 1.39 (t, 9H, $CH_2$). $^{13}$C NMR (400 MHz, $CDCl_3$): $\delta$ 193.69 (C=S), 180.58(C=O), 176.74(C=O), 148.65(C-N), 134.96, 134.81, 132.73, 132.65, 132.52, 132.36, 129.87, 126.73, 56.77, 56.19, 56.05, 53.45, 52.37, 50.26, 45.90, 41.05, 40.88.

### 4B.4.4. Synthesis of metal complexes 1-5

The ligand precursors 2-chloro-3-{2-(piperazinyl)ethyl}-amino-1, 4-naphthoquinone (**L**) (0.319 g, 1.0 mmol) was dissolved in 20 ml of triethyl amine and after 30 minutes $CS_2$ (0.114 g, 1.5 mmol) were added. The reaction mixture was stirred rigorously for one hour at room temperature. During this time, a change in colour from to pale yellow was observed, indicating the formation of 2-chloro-3-{2-(piperazinyl)ethyl}-amino-1, 4-naphthoquinone dithiocarbamato ligand. This ligand was allowed to react *in situ* generation of the dithiocarbamato ligand to the $Mn(OAc)_2.4H_2O$ (0.081 g, 0.33

mmol), $Co(OAc)_2.4H_2O$ (0.084 g, 0.33 mmol), $Ni(OAc)_2.4H_2O$ (0.124 g, 0.5 mmol), $Cu(OAc)_2.H_2O$ (0.101 g, 0.5 mmol) and $Zn(OAc)_2.2H_2O$ (0.110 g, 0.5 mmol) metal salts. The mixture was stirred 6-7 hrs then precipitate comes. Filter it and wash the residue with petroleum ether and distilled water three to four times. Collect the residue and after drying in high vacuum store the solid powder in 10-20 ºC under nitrogen atmosphere.

1. Light pink solid (0.380 g, 92% yield); m.p. >325°C (decomposes); IR (KBr): υ = 3265 (N-H), 2940 (C-H), 1676 (C=O), 1427 (C=N), 1010 (C–S) $cm^{-1}$; elemental analysis calcd (%) for $C_{51}H_{51}Cl_3N_9O_6S_6Mn$ (M. Wt. 1239.6): C 49.41, H 4.15, N 10.17, S 15.52; found: C 49.64, H 4.09, N 10.05, S 15.94.
2. Brown solid (0.352 g, 85% yield); m.p. 270°C (decomposes); IR (KBr): υ = 3324 (N-H), 2933 (C-H), 1675 (C=O), 1490 (C=N), 1007 (C–S) $cm^{-1}$; elemental analysis calcd (%) for $C_{34}H_{34}Cl_2N_6O_4S_4Co$ (M. Wt. 1243.6): C 49.25, H 4.13, N 10.14, S 15.47; found: C 49.34, H 4.05, N 10.02, S 15.41. NMR could not be recorded due to poor solubility in DMSO even after acidification.
3. Dark Brown solid (0.314 g, 74% yield); m.p. 315°C (decomposes); $^1$H NMR (400 MHz, $CDCl_3$): $\delta$ 8.18-8.16 (d, 2H, *Ph*), 8.05-8.03 (d, 2H, *Ph*), 7.75-7.73 (dd, 2H, *Ph*), 7.65-7.64 (dd, 2H, *Ph*), 6.79( s, 2H, *N-H*), 4.00 (d, 2H, $CH_2$), 3.86 (d, 4H, $CH_2$), 3.62-3.60 (d, 6H, $CH_2$), 3.14-3.12 (d, 6H, $CH_2$), 2.75 (d, 2H, $CH_2$), 2.60 (d, 4H, $CH_2$). IR (KBr): υ = 3328 (N-H), 2911 (C-H), 1676 (C=O), 1440 (C=N), 1006 (C–S) $cm^{-1}$; elemental analysis calcd (%) for $C_{34}H_{34}Cl_2N_6O_4S_4Ni$ (M. Wt. 848.5): C 48.13, H 4.04, N 9.90, S 15.12; found: C 48.34, H 4.05, N 9.85, S 15.21. $^{13}$C NMR could not be recorded due to poor solubility in DMSO even after acidification.
4. Dark Brown solid (0.341 g, 80% yield); m.p. 245°C (decomposes); IR (KBr): υ = 3331 (N-H), 2928 (C-H), 1676 (C=O), 1498 (C=N), 1007 (C–S) $cm^{-1}$; elemental analysis calcd (%) for $C_{34}H_{34}Cl_2N_6O_4S_4Cu$ (M. Wt. 853.4): C 47.85, H 4.02, N 9.85, S 15.03; found: C 47.98, H 4.08, N 10.05, S 15.18.
5. Reddish Yellow solid (0.380 g, 89% yield); m.p. 216°C (decomposes); $^1$H NMR (400 MHz, $CDCl_3$): $\delta$ 8.18-8.16 (dd, 2H, *Ph*), 8.06-8.04 (dd, 2H, *Ph*), 7.77-7.74 (td, 2H, *Ph*), 7.68-7.66 (td, 2H, *Ph*), 6.78( s, 2H, *N-H*), 4.18(m, 8H, $CH_2$), 4.02 (t, 4H, $CH_2$), 2.78-2.66(m, 12H, $CH_2$). $^{13}$C NMR (400 MHz, $CDCl_3$): $\delta$ 203.08(C=S), 180.85(C=O), 176.77(C=O), 155.19(C-N) 147.84(C-N), 144.50(C-N), 134.97,

134.81, 132.66, 132.53, 129.84, 126.84, 126.7, 56.02, 54.73, 52.00, 51.81, 51.10, 40.89; $^{13}$C DEPT 135 NMR (400 MHz, $CDCl_3$): $\delta$ 134.97, 132.56, 126.84, 126.60, 56.02, 51.82, 51.10, 51.00, 40.90. IR (KBr): $\upsilon$ = 3313 (N-H), 2966 (C-H), 1677 (C=O), 1434 (C=N), 1008 (C–S) $cm^{-1}$; elemental analysis calcd (%) for $C_{34}H_{34}Cl_2N_6O_4S_4Zn$ (M. Wt. 855.2): C 47.75, H 4.01, N 9.83, S 15.00; found: C 47.95, H 4.03, N 10.01, S 15.01.

## 4B.5. References


1. Coucouvanis, D. *Prog. Inorg. Chem*. **1979**, *26*, 301.
2. Clemenson, P. I. *Coord. Chem. Rev.* **1990**, *106*, 171.
3. Bousseau, M.; Valade, L.; Legros, J. P.; Cassoux, P.; Garbaukas, M.; Interrante, L. V. *J. Am. Chem. Soc.* **1986**, *108*, 1908.
4. Cassoux, P.; Valade, L.; Kobayashi, H.; Kobayashi, A.; Clark, R. A.; Underhill, A. E. *Coord. Chem. Rev.* **1991**, *110*, 115.
5. Kobayashi, A.; Fujiwara, E.; Kobayashi, H. *Chem. Rev*. **2004**, *104*, 5243.
6. Coomber, A. T.; D. Beljonne, Friend, R. H.; Bredas, J. L.; Charlton, A.; Robertson, N.; Underhill, A. E. *Nature* **1996**, *380*, 144.
7. Coomber, A. T.; Beljonne, D.; Friend, R. H.; Bredas, J. L.; Charlton, A.; Robertson, N.; Underhill, A. E.; Kurmoo, M.; Day, P. *Nature* **1996**, *380*, 144.
8. (a) Singh, N.; Singh, B. *Bull. Chem. Soc. Jpn.* **2008**, *81*, 262; (b) Singh, N.; Prasad, A.; Sinha, R. K. Bull. Chem. Soc. Jpn. **2009**, *82*, 81.
9. Yan, Y.; Krishnakumar, S.; Yu, H.; Ramishetti, S.; Deng, L. –W.; Wang, S.; Huang, L.; Huang, D. *J. Am. Chem. Soc*. **2013**, *135*, 5312.
10. (a) Singh, N.; Kumar, A.; Prasad, R.; Molloy, K. C.; Mahon, M. F. *Dalton Trans*. **2010**, *39*, 2667; (b) Singh, V.; Chauhan, R.; Gupta, A. N.; Kumar, V.; Drew, M. G. B.; Bahadur L.; Singh, N. *Dalton Trans*. **2014**, *43*, 4752.
11. (a) Wilton-Ely, J. D .E. T.; Solanki, D.; Knight, E. R.; Holt, K. B.; Thompson, A. L.; Hogarth, G. *Inorg. Chem*. **2008**, ***47***, 9642; (b) Wilton-Ely, J. D. E. T.; Solanki, D.; Hogarth, G. *Eur. J. Inorg. Chem.* **2005**, 4027; (c) Wong, W. W. H.; Curiel, D.; Lai, S. -W.; Drew, M. G. B.; Beer, P. D. *Dalton Trans*. **2005**, 774.
12. Tisdale, W. H.; Williams, I. *Disinfectant*, US197296, 1934.
13. (a) Kumar, L.; Sarswat, A.; Lal, N.; Sharma, V. L.; Jain, A.; Kumar, R.; Verma, V.; Maikhuri, J. P.; Kumar, A.; Shukla, P. K.; Gupta, G. *Eur. J. Med. Chem*. **2010**,

*45*, 817; (b) Jangir, S.; Bala, V.; Lal, N.; Kumar, L.; Sarswat, A.; Kumar, L.; Kushwaha, B.; Singh, P.; Shukla, P. K.; Maikhuri, J. P.; Gupta, G.; Sharma, V. L. *Org. Biomol. Chem*. **2014**, *12*, 3090; (c) Wood, T. F.; Gardner, J. H. *J. Am. Chem. Soc*. **1941**, *63*, 2741; (d) Kapa, N. C.; Muccioli, G. G.; Labar, G.; Poupaert, J. H.; Lambert, D. M. *J. Med. Chem*. **2009**, *52*, 7310; (e) Huang, W.; Ding, Y.; Miao, Y.; Liu, M. -Z.; Li, Y.; Yang, G. -F. *Eur. J. Med. Chem*. **2009**, *44*, 3687.

14. (a) Sharma, A. K. *Thermochim. Acta* **1986**, *104*, 339; (b) Hill, J. O.; Murray J. P.; Patil, K. C. *Rev. Inorg. Chem*. **1994**, *14*, 363.
15. (a) Powis, G. *Pharmacol. Ther*. **1987**, *35*, 57; (b) O'Brien, P. J. *Chem. Biol. Interact*. **199**1, *80*, 1.
16. (a) Hoover, J. R. E.; Dag, A. R. *J. Am. Chem. Soc.*, **1954**, *76*, 4148; (b) Clark, N. G. *Pestic. Sci.* **1985**, *16*, 23; (c) Kobayashi, K.; Umakoshi, H.; Matsunaga, A.; Tanmatsu, M.; Morikawa, O.; Konishi, H. *Bull. Chem. Soc. Jpn*. **2004**, *77*, 2095; (d) Shimbashi, A.; Tsuchiya, A.; Imoto, M.; Nishiyama, S. *Bull. Chem. Soc. Jpn*. **2004**, *77*, 1925; (e) Tandon, V. K.; Maurya, H. K.; Tripathi, A.; ShivaKesva, G. B.; Shukla, P. K.; Srivastava, A.; Panda, D. *Eur. J. Med. Chem*. **2009**, *44*, 1086; (f) Biot, C.; Bauer, H.; Schirmer, R. H.; Charret, E. D. *J. Med. Chem*. **2004**, *47*, 5972; (g) Pardee, A. B.; Li, Y. Z.; Li, C. J. *Cancer Drug Targets* **2002**, *2*, 227; (h) Hazra, B.; Sarma, M. D.; Sanyal, U. *J. Chromatogr. B Anal. Technol. Biomed. Life Sci*., **2004**, *812*, 259.
17. (a) Anastasiadis, C.; Hogarth, G.; Wilton-Ely, J. D. E. T. *Inorg. Chim. Acta* **2010**, *363*, 3222; *and the references cited in*.; (b) Wilton-Ely, J. D. E. T. *Dalton Trans*. **2008**, *25*; Knight, E. R.; Leung, N. H.; Thompson, A. L.; Hogarth, Wilton-Ely, G. J. D. E. T. *Inorg. Chem*. **2009**, *48*, 3866; (c) Cookson, J. Beer, P. D. *Dalton Trans*. **2007**, 1459.
18. Verma, S. K.; Singh, V. K. *J. Coord. Chem.* **2015**, 1-16. DOI: 10.1080/00958972.2014.1003550.
19. Wilton-Ely, J. D. E. T.; Solanki, D.; Knight, E. R.; Holt, K. B.; Thompson, A. L.; Hogarth, G. *Inorg. Chem*. **2008**, *47*, 9642;
20. (a) Mamba, S. M.; Mishra, A. K.; Mamba, B. B.; Njobeh, P. B.; Dutton, M. F.; Kankeu, E. F. *Spectrochimica Acta Part A* **2010**, *77*, 579; (b) Verma, S. K.; Singh, V. K. *Polyhedron* **2014**, *76*, 1.

21. Bharti, A.; Bharati, P.; Chaudhari, U. K.; Singh, A.; Kushawaha, S. K.; Singh, N. K.; Bharty, M. K. *Polyhedron* **2015**, *85*, 712.
22. Pawar, O.; Patekar, A.; Khan, A.; Kathawate, L.; Haram, S.; Markad, G.; Puranik, V.; Gawali, S. S. *J. Mol. Struct.* **2014**, *1059*, 68.
23. (a)Perpete, E. A.; Lambert, C.; Wathelet, V.; Preat, J.; Jacquemin, D. *Spectrochim. Acta A* **2007**, *68*, 1326; (b) Leyva, E.; Lopez, L. I.; Carrillo, S. E. L.; Kessler, M. R.; Rojas, A. M. *J. Fluorine Chem*. **2011**, *132*, 94; (c) Leyva, E.; Sobeck, S. J. S.; Carrillo, S. E. L.; Lara, D. A. M. *J. Mol. Struct*. **2014**, *1068*, 1.
24. (a) Shyamala, B. S.; Lakshmi, P. V. A.; Raju. V. J. *J. Sci. Res*. **2010**, *2*, 525; (b) Riveros, P. C.; Perilla, I. C.; Poveda, A.; Keller, H. J.; Pritzkow, H. Polyhedron, **2000**, *19*, 2327; (c) B. F. G.; Johnson, K. H.; Al-Obalidi, J. A. Mecleverty, *J. Am. Chem. Soc. A*, **1969**, *19*, 1668; (d) Anderson, R. J.; Bendell, D. J.; Groundwater, P. W. Organic Spectroscopic Analysis; RSC: Cambridge, UK 2004; (e) Wong,; W. W. H.; Phipps, D. E.; Beer, P. D. *Polyhedron* **2004**, *23*, 2821; (f) Gölcü, A.; Yavuz, P.; *Russ. J. Coord. Che*m. **2008**, *34*, 106; (g) Vanthoeun, K.; Yamazaki, H.; Suzuki, T.; Kita, M. *J. Coord. Che*m. **2013**, *66*, 2378; (h) Jeffrey, N. K.; James, F. S. *Anal. Chem.* **1987**, *59*, 703.
25. Win, T.; Bittner, S. *Tetrahedron Lett*. **2005**, *46*, 3229.
26. Vanthoeun, K.; Yamazaki, H.; Suzuki, T.; Kita, M. *J. Coord. Che*m. **2013**, *66*, 2378;
27. King, J. N.; Fritz, J. S. *Anal. Chem.* **1987**, *59*, 703.
28. Hendrickson, R.; Martin, R. L.; Rohde, N. M. Inorg. Chem. **1974**, *13*, 1933 *and the references cited in*.
29. Cambi, L.; Cagnasso, A. *Atti. Accad. Naz. Lincei, C1. Sci. Fis. Mat. Nat., Rend*. **1931**, *13*, 404.
30. Preti, C.; Tosi, G.; Zannini, P. *J. Mol. Struct.* **1980**, *65*, 283.
31. Pandey, R.; Kumar, P.; Singh, A. K.; Shahid, M.; Li, P.-z.; Singh, S. K.; Xu, Q.; Misra, A.; Pandey, D. S. *Inorg. Chem.* **2011**, *50*, 3189.
32. Kumar, V.; Singh, V.; Gupta, A. N.; Singh, S. K.; Drew, M. G. B.; Singh, N. *Polyhedron* **2015**, *89*, 304.
33. Verma, S. K.; Kadu, R.; Singh, V. K. *Synth. React. Inorg. Met.-Org. Nano-Met. Chem*. **2014**, *44*, 441.

34. Kumar, A.; Chauhan, R.; Molloy, K. C.; Kociok-Kçhn, G.; Bahadur, L.; Singh, N. *Chem. Eur. J.* **2010**, *16*, 4307.
35. Huang, C. M.; Chen, C. H.; Pornpattananangkul, D.; Zhang, L.; Chan, M.; Hsieh, M. F.; Zhang, L. *Biomaterials* **2011**, *32*, 214.
36. Monk, B. C.; Goffeau, A. *Science* **2008**, *321*, 367.
37. National Committee for Clinical Laboratory Standards, Performance Standards for Antimicrobial Susceptibility Testing, 8th Informational Supplement. M100 S12, National Committee for Clinical Laboratory Standards, Villanova, Pa, 2002.
38. Pellerito, C.; Nagy, L.; Pellerito, L.; Szorcsik, A. *J. Organomet. Chem*. **2006**, *691*, 1733.
39. (a) van den Bossche, H.; Dromer, F.; Improvissi, L.; Lozane-Chiu, M.; Hex, J. H.; Sanglard, D. *Medical Mycology*, **1998**, *36*, 119; (b) Mohammad, A.; Varshney, C.; Nami, S. A. A. *Spectrochimica Acta Part A*, **2009** , *73*, 20.

## 4B.6. Spectra

### 4B.6.1. NMR spectra

The NMR spectra of the 2-chloro-3-{2-(piperazinyl)ethyl}-amino-1, 4-naphthoquinone (**L**), its triethyl ammonium dtc salt and complexes are summarized below as Figure S7 to Figure S12.

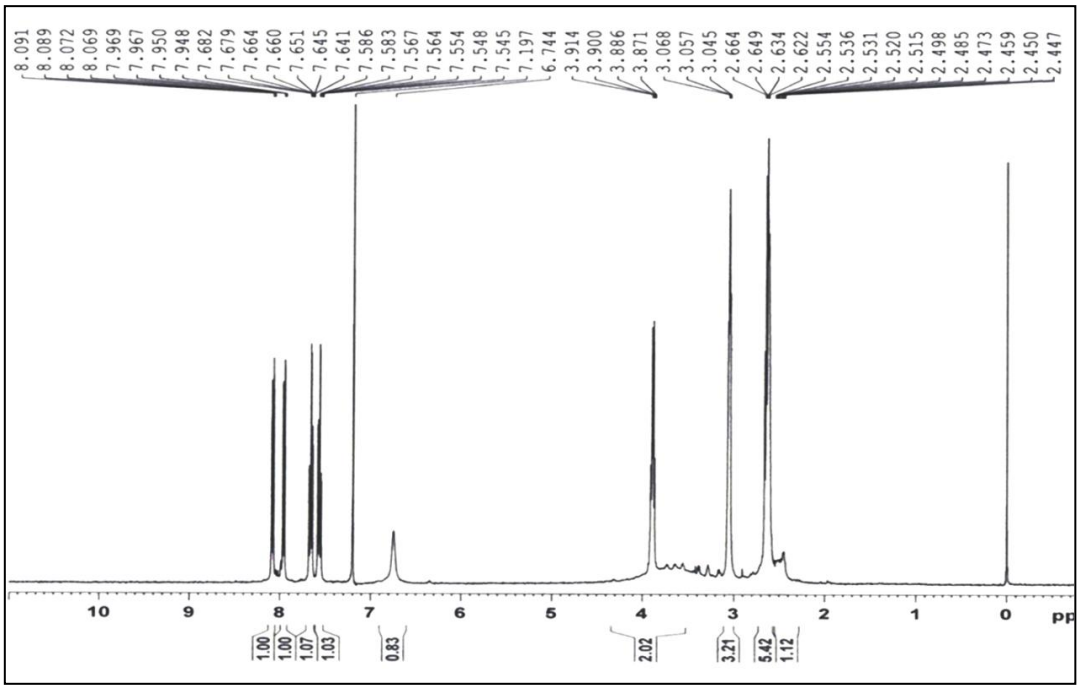


**Figure S7**. $^{1}$H NMR spectrum of the 2-chloro-3-{2-(piperazinyl)ethyl}-amino-1, 4-naphthoquinone (**L**).

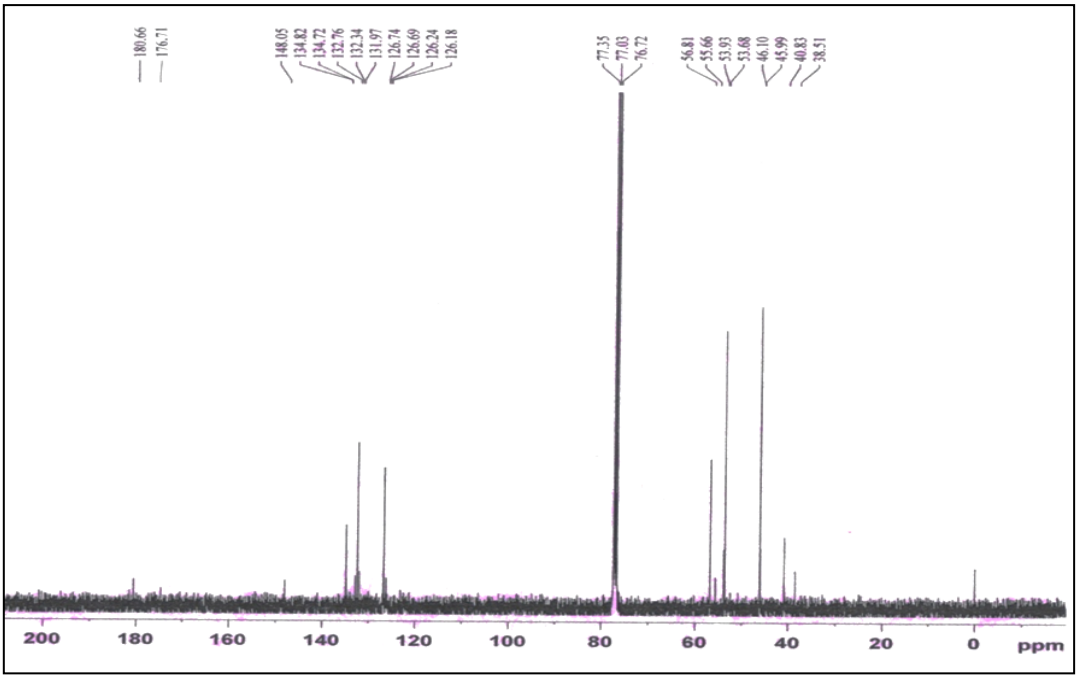


**Figure S8**. $^{13}$C NMR spectrum of 2-chloro-3-{2-(piperazinyl)ethyl}-amino-1, 4-naphthoquinone (**L**).

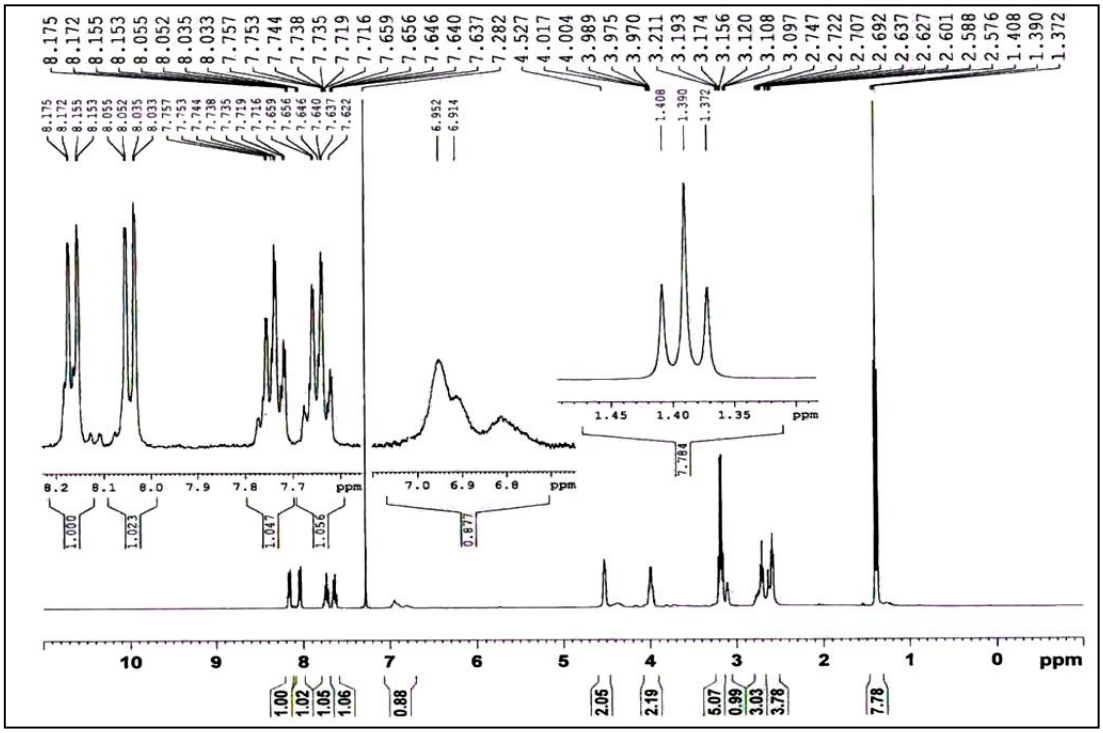


**Figure S9**. $^{1}$H NMR spectrum of triethyl ammonium dtc salt of the ligand precursor L.

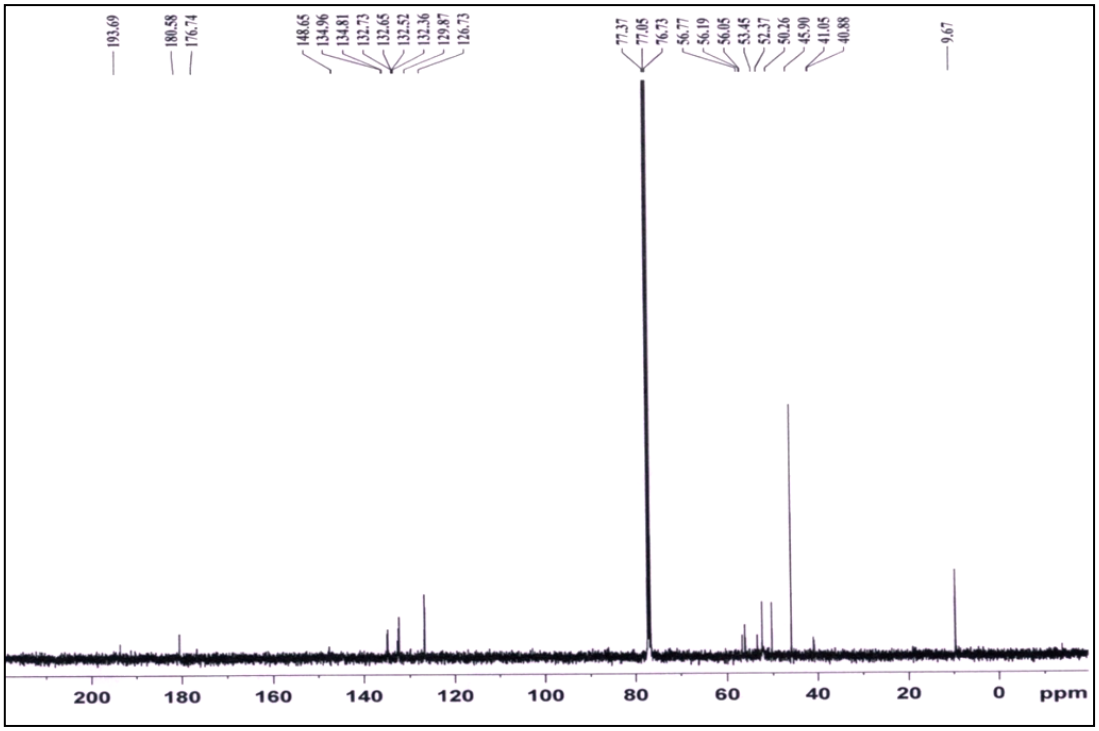


**Figure S10**. $^{13}$C NMR spectrum of triethyl ammonium dtc salt of the ligand precursor L.

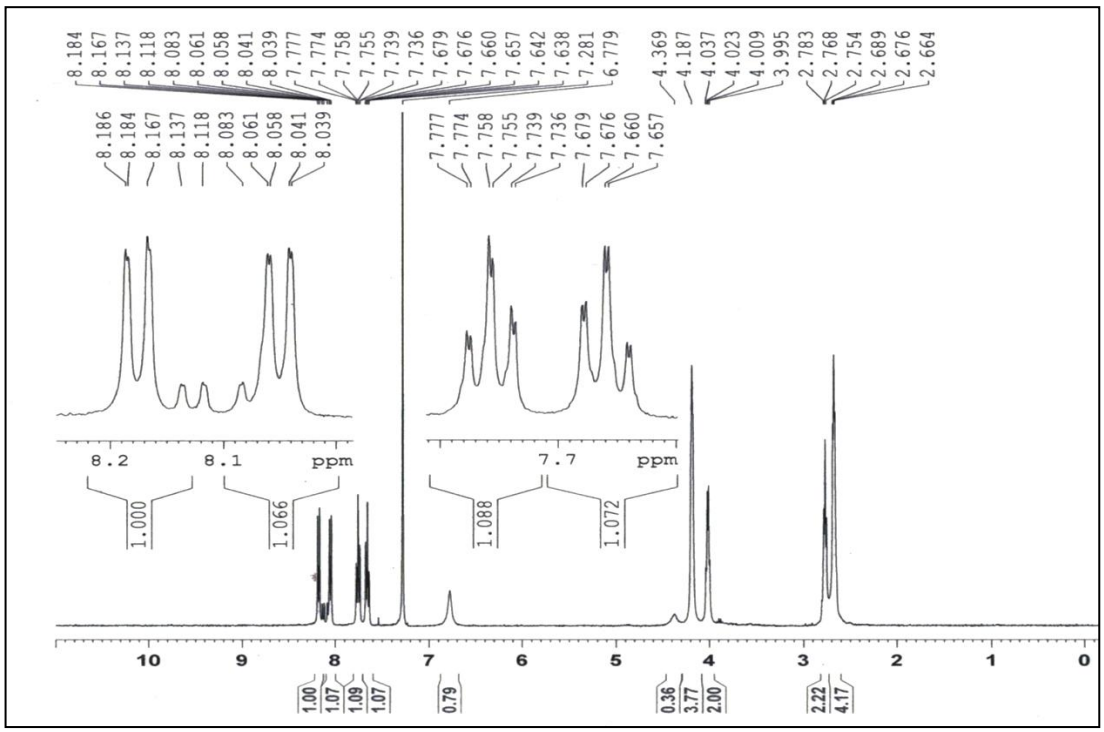


**Figure S11**. $^{1}$H NMR spectrum of compound 5.

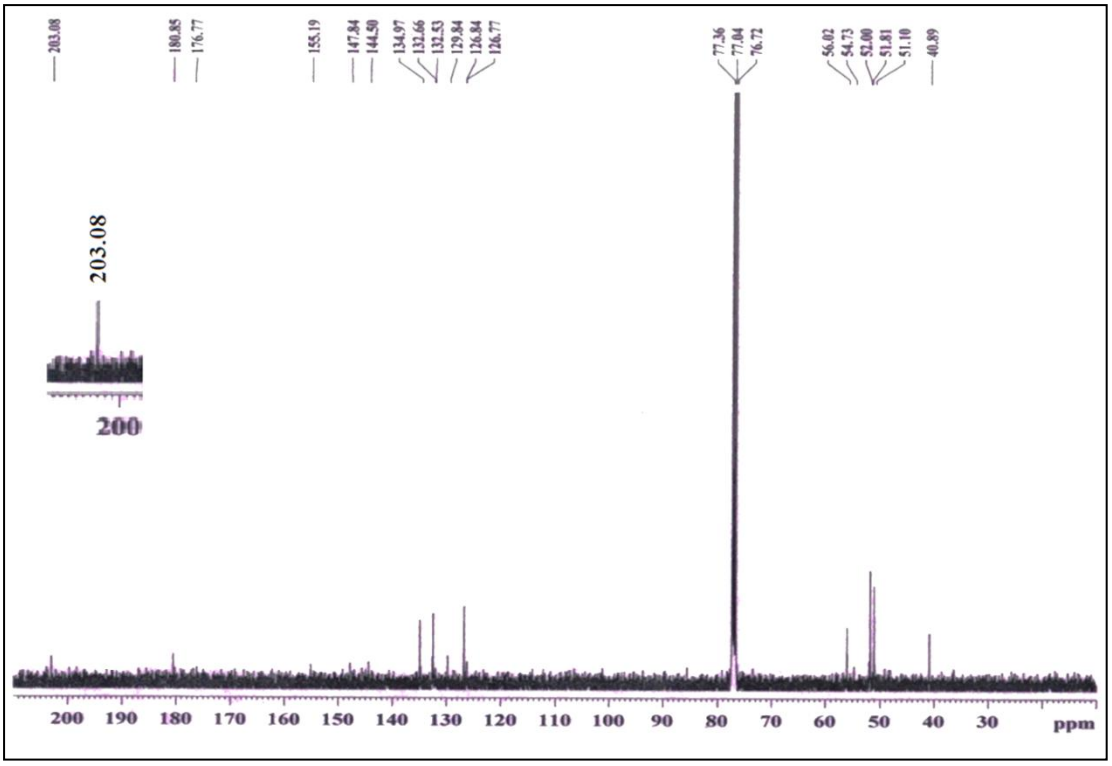


**Figure S12**. $^{13}$C NMR spectrum of compound 5.

### 4B.6.2. ESI MS spectra

The ESI MS spectra of the dithiocarbamate metal complexes are summarized below as Fig. S13 to S14

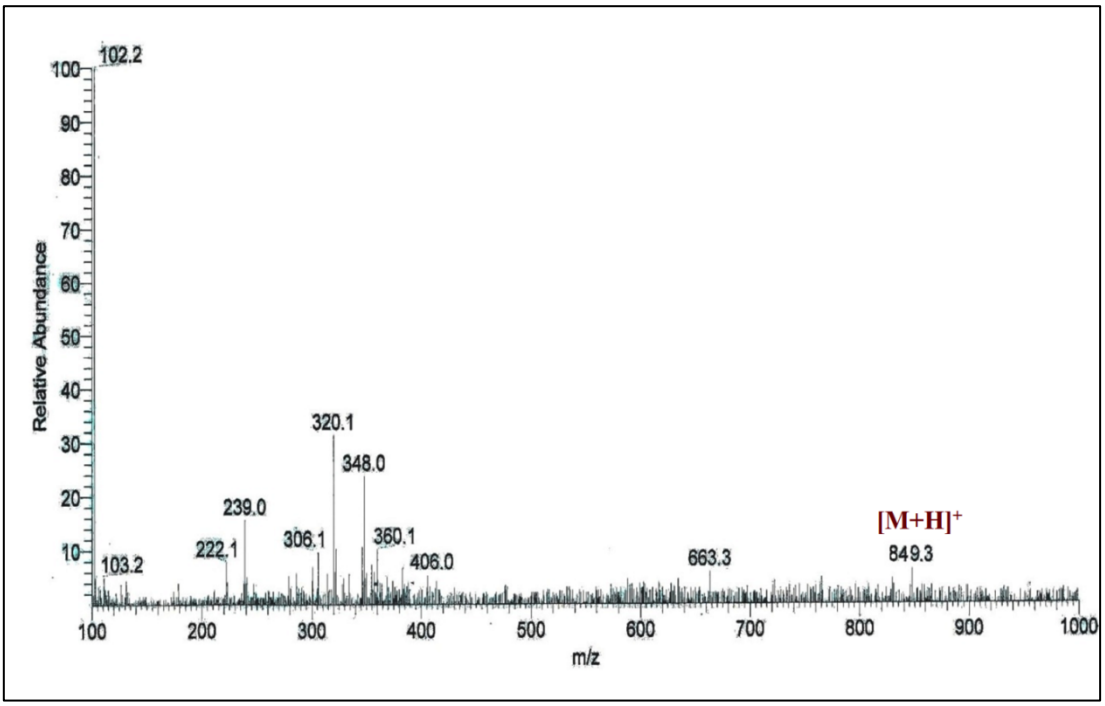


**Figure S13**. ESI MS spectra of compound **3**.

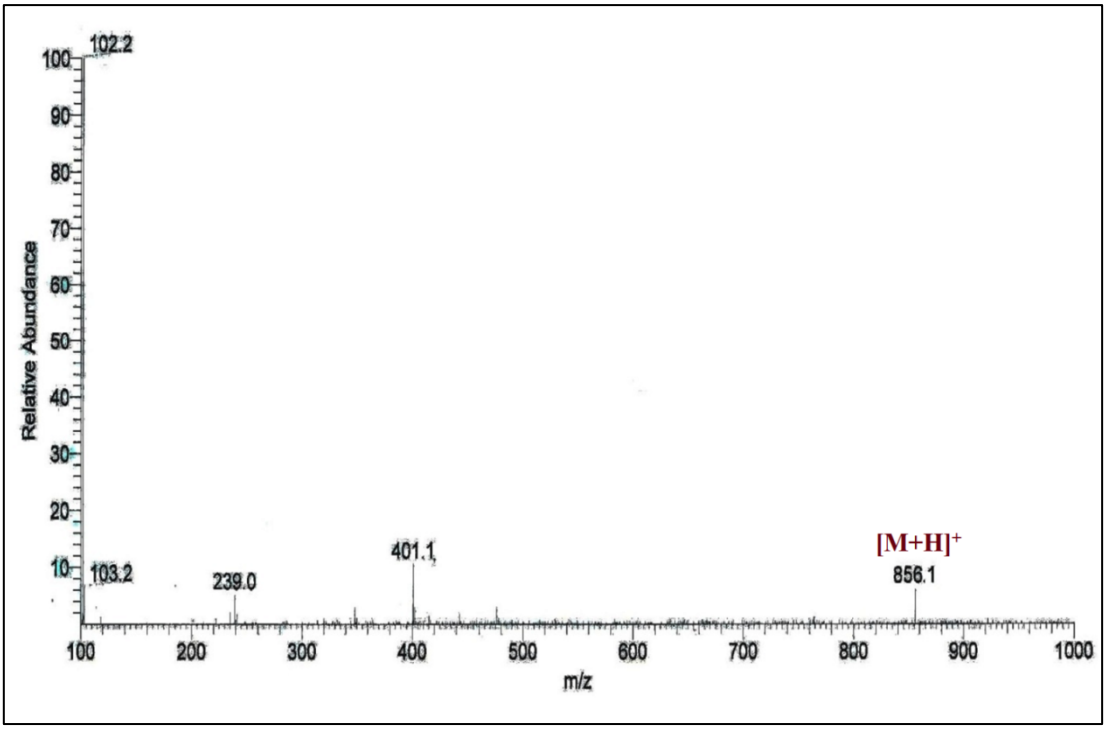


**Figure S14**. ESI MS spectra of compound 5.

### 4B.6.3. TG/DTA

TG/ DTA curve of the dithiocarbamate metal complexes are summarized below as Figure S15 to Figure S16.

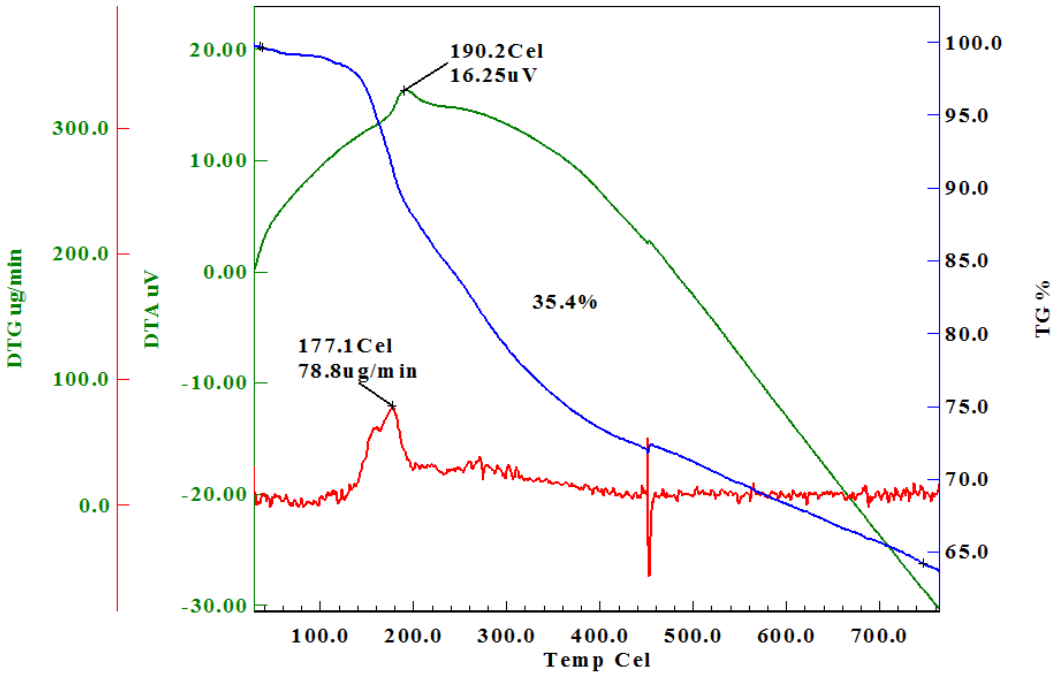


**Figure S15**. TG/DTA curve of the dithiocarbamate metal complex **1**